IOP Publishing Journal of Optics
J. Opt. 19 (2017) 105506 (11pp) https://doi.org/10.1088/2040-8986/aa8502

Binary-phase compression of stretched pulses

Vadim V Lozovoy[1], Muath Nairat[1] and Marcos Dantus[1,2]

[1] Department of Chemistry, Michigan State University, East Lansing, MI-48824, United States of America
[2] Department of Physics and Astronomy, Michigan State University, East Lansing, MI-48824, United States of America

E-mail: dantus@msu.edu

Received 8 March 2017, revised 24 July 2017
Accepted for publication 8 August 2017
Published 20 September 2017

Abstract

Pulse stretching and compression are essential for the energy scale-up of ultrafast lasers. Here, we consider a radical approach using spectral binary phases, containing only two values (0 and π) for stretching and compressing laser pulses. We numerically explore different strategies and present results for pulse compression of factors up to a million back to the transform limit and experimentally obtain results for pulse compression of a factor of one hundred, in close agreement with numerical calculations. Imperfections resulting from binary-phase compression are addressed by considering cross-polarized wave generation filtering, and show that this approach leads to compressed pulses with contrast ratios greater than ten orders of magnitude. This new concept of binary-phase stretching and compression, if implemented in a multi-layer optic, could eliminate the need for traditional pulse stretchers and more importantly expensive compressors.

Keywords: ultrafast amplification, chirp, pulse compression, femtosecond

(Some figures may appear in colour only in the online journal)

1. Introduction

Energy scale-up of ultrafast laser sources relies on the temporal stretching of pulses prior to amplification via chirped pulse amplification (CPA) [1]. As ultrafast sources gain acceptance in medicine and industry, the cost and robustness of pulse compressors are parameters in need for optimization. Similarly, as lasers with pulse energies in the hundreds or even the thousands of joules would be considered, the compressors for those sources are extremely expensive because of the need for gratings and mirrors with areas exceeding 1 m^2 that require precise alignment inside vacuum chambers. In view of this technical challenge, we question if there are alternative approaches to pulse compression. Given that pulse compression is a process that brings into phase all the frequencies within the spectrum of the pulse, we consider a frequency domain approach in which out-of-phase components are brought into phase by a π step. The resulting binary spectral phases, containing values of zero and π, are then evaluated for their ability to compress pulses.

The fact that destructive interference is what leads to pulse stretching has been known for some time; here we reference early work where blocking certain regions of the spectrum led to an increase in the second harmonic generation [2] via an approach that was analogous to Fresnel zone plates [3–5]. In general, the delivery of large negative dispersion is analogous to creating a large lens, which was solved by the Fresnel lens.

Our work involves numerical calculations and experimental measurements taking advantage of a pulse shaper [6] that is calibrated and controlled by the multiphoton intrapulse-interference phase scan (MIIPS) (BioPohotonic Solutions Inc.) software [7–9]. Our work is a continuation of efforts from our group to explore new methods to mitigate nonlinear optical effects in femtosecond laser amplifiers via the introduction of binary spectral phases [10] or via the generation of square pulses [11]. The quality of our results, especially when combined with cross-polarized wave generation filtering [12], should inspire a new generation of optics along the lines of chirped mirrors [13] and volume Bragg gratings [14] that take advantage of our approach.

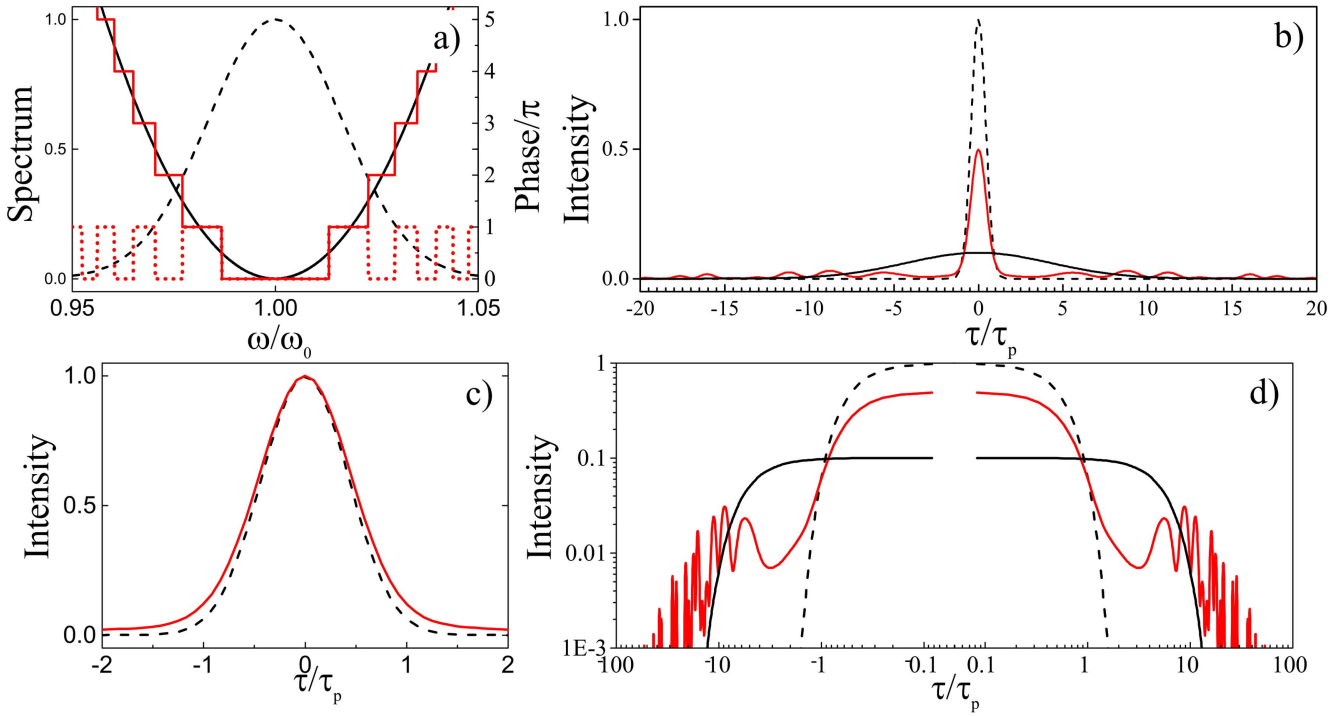

Figure 1. Principle of binary-phase compression. (a) (*x*-axis is relative to the carrier frequency) Spectrum (dashed black) with a parabolic phase (black solid) dispersion to stretch the pulse, phase to compensate back to TL duration (red solid and dotted). (b) (*x*-axis is ratio of time to the duration of the pulse) On the *y* axis are the intensities of the TL (dashed), chirped (black) and compressed (red) pulses. (c) Intensities of TL (dashed) and compressed (red) pulses normalized on max. (d) Plots of the same pulses as in (b) plotted on a log–log scale to show the intensities of the stretched laser pulses at long times.

2. Principle of stretching and compression

Here we begin by reviewing some basic formulas before we introduce the concept of binary phase compression. The electric field strength in the time domain $E(t)$ can be represented as a Fourier integral of the complex spectrum $E(\omega)$

$$\tilde{E}(t) \propto E(t) + \text{c.c.} = \int E(\omega) e^{-i\omega t} d\omega + \text{c.c.}, \quad (1)$$

where the spectral phase $\varphi(\omega)$ controls the time dependence of the field $|E(\omega)|$ according to

$$E(t) = \int |E(\omega)|\, e^{i\varphi(\omega)} e^{-i\omega t} d\omega. \quad (2)$$

Temporal pulse stretching is typically accomplished through the introduction of chirp, which corresponds to the introduction of a quadratic spectral phase

$$\varphi(\omega) = \tfrac{1}{2}\varphi''(\omega - \omega_0)^2. \quad (3)$$

If the pulse spectrum has a Gaussian shape (dashed line in figure 1(a))

$$|E(\omega)| = \exp\left[-\tfrac{1}{2}\tau_0^2(\omega - \omega_0)^2\right], \quad (4)$$

then the transform limited (TL) pulse in the time domain has a Gaussian shape with pulse duration given by $\tau_0 = \tau/2\sqrt{\ln(2)} \cong 0.601\tau$, where τ is the full width at half maximum (FWHM), such that

$$|E(t)| = \exp\left[-\tfrac{1}{2}t^2\tau_0^{-2}\right]. \quad (5)$$

Temporal pulse stretching by N times requires a chirp of value $\varphi'' = N\tau_0^2$ (black line in figure 1(a)) corresponding to the complex spectral field

$$E(\omega) = \exp\left[-\tfrac{1}{2}\tau_0^2(\omega - \omega_0)^2\right]\exp\left[-i\tfrac{N}{2}\tau_0^2(\omega - \omega_0)^2\right]. \quad (6)$$

The temporal intensity profile of this pulse is stretched and its peak intensity drops by N times (black line in figure 1(b))

$$I(t) \cong \left(\frac{I_{\max}}{N}\right)\exp\left[-\frac{t^2}{N^2\tau_0^2}\right]. \quad (7)$$

It is instructive to analyze how different spectral components add up together to produce the stretched pulse. We note there are spectral regions where the phase difference between spectral components equals π. These components are out of phase, or in other words, they have opposite signs because $e^{i\pi} = -1$. For large chirp values, there are many close spectral components of approximately equal amplitude with opposite signs that destructively interfere, therefore the peak intensity decreases and the pulse is stretched.

To compress such a chirped stretched pulse, one typically would introduce a phase with the opposite chirp sign. Here, we propose a coarse approach that changes the phase only for the frequency components that are out of phase. To

accomplish this, we find the frequencies that are out of phase, i.e. their phase equals $n\pi$, with n being an odd number. For those frequencies we add (or subtract) a π phase value to cause them to constructively interfere. When n is an even number, the phase is kept without change. Such binary-phase compression is shown in figure 1(a) (red line). The 'staircase' looking line crosses the spectral phase being compressed at frequencies where the phase equals $n\pi$. The dotted red line corresponds to a different representation of the same phase (red line) because phase is a cyclic function with a period of 2π. Hence, any odd $n\pi$ can be replaced with π whereas even $n\pi$ are replaced with 0. Applying this phase compresses the pulse in the time domain, as shown in figure 1(b). The red line corresponds to the binary-phase compressed pulse (chirped and binary-phase compressed). When normalized to unit intensity, the TL pulse (black dashed line) in figure 1(c) is very close to the profile of the stretched and binary-phase compressed pulse. For this example, the pulse was stretched only by a factor of 10; when plotted in logarithmic scale, figure 1(d), the chirped pulse (black line) has a 10 times smaller peak intensity than the TL pulse (dashed line). The amplitude of the binary-phase compressed pulse (red line) is about 0.5 from the maximum; the compressed pulse duration at FWHM is very close to the TL pulse. Because we use pure phase modulation in this example, approximately half of the energy is not lost but actually spread over very long times. This energy looks like noise beyond the chirped pulse duration as depicted in the log–log plot in figure 1(d). Below we present experimental binary-phase compression and then discuss in detail why, in our opinion, it deserves more than pure academic interest.

3. Experiment

The expressions provided above have been implemented in the laboratory using a calibrated pulse shaper capable of compressing the pulses to within 0.1% of the theoretical TL. Pulse compression was based on the MIIPS approach [7–9]. The experimental setup consists of a regeneratively amplified Ti:sapphire laser (Spitfire, Spectra Physics Inc.) producing 1 mJ pulses at 1 kHz. The output was split, reserving one arm for a cross-correlation setup. The main portion of the beams was directed to the pulse shaper (MIIPS-HD, BioPhotonic Solutions Inc. USA). Both beams were then focused non-collinearly into a nonlinear crystal (BBO) using a 300 mm focal length achromatic lens. The second-harmonic signal was recorded with a spectrometer (USB 4000, Ocean Optics) as a function of time delay to produce the cross-correlation function. Cross correlations were measured using a Mach–Zehnder interferometer in which one arm 'as-is' (reference arm) and applying the phase mask to the other arm (the pulse shaper arm). The scans were realized for TL pulses, as well as for chirped pulses stretched by a factor of 10 and 100, using a quadratic phase with values of 10 000 fs^2 and 100 000 fs^2, respectively, and for the same stretched pulses after adding the binary-phase compression mask as prescribed above. Technically speaking, the binary compression mask was added to the stretching mask. It is worth noting that the currently shown binary compression was applied to pulses that were stretched using a quadratic phase mask, however, other phase masks as well as other stretching forms such as dissipative solitons [15, 16] are still amenable to our concept as shown below.

Experimental results are presented in figure 2. The spectrum of the amplified laser is shown as a dashed line in figure 2(a). The pulses are stretched by a factor of 10 using chirp (parabolic black line) and compressed by a binary-phase function (staircase red line). Cross correlation measurements of the TL pulses (black dashed line), stretched pulses (black line), and binary-phase compressed pulses (red line) are shown in figure 2(b). The quality of the compressed pulses is shown in figure 2(c), where the TL pulses are shown (black dashed line), along with the binary-phase compressed pulses after being stretched by a factor of 10 (red line) and 100 (blue line). Notice that the TL pulses show that the reference pulse used for the cross correlation measurements has a small amount of negative third-order dispersion ($\sim -10^3$ fs^3). The overall experimental performance of binary-phase compression can be appreciated in figure 2(d), where the duration of the pulses stretched by a factor of 10 (red) and 100 (blue) are shown in the log–log scale before (dashed) and after (line) compression. We find that the experimental results confirm that binary-phase compression can recover the original pulse duration. The only drawback is the amplitude loss due to the residual destructive interference, which reduces the throughput to about 40%. While traditional grating stretchers and compressors have a typical throughput of about 50%, but can be designed to have higher throughput.

4. Numerical simulations

The successful experiments for 10× and 100× stretched pulses using binary-phase compression prompt us to compare different binary-phase and amplitude compression approaches. It is also important to evaluate binary-phase compression using different input pulse spectra. The practical implementation of this approach requires evaluation for very large stretching factors, up to a factor of a million. Experimental implementation will inevitably suffer from imperfections in the delivery of the binary compression spectral phase, in particular lack of experimental accuracy and precision. We performed numerical simulations that include some of the most common imperfections expected in the experimental implementation. Finally, as we envision the applicability in implementing the binary-phase compression for high-energy pulses, we address the contrast ratios that can be achieved by binary-phase compression in combination with nonlinear filtering.

4.1. Different methods of compression

Starting with a pulse having a Gaussian spectrum equation (4) and assuming that the stretched pulse is chirped equation (3), then it is possible to write an analytical formula for the

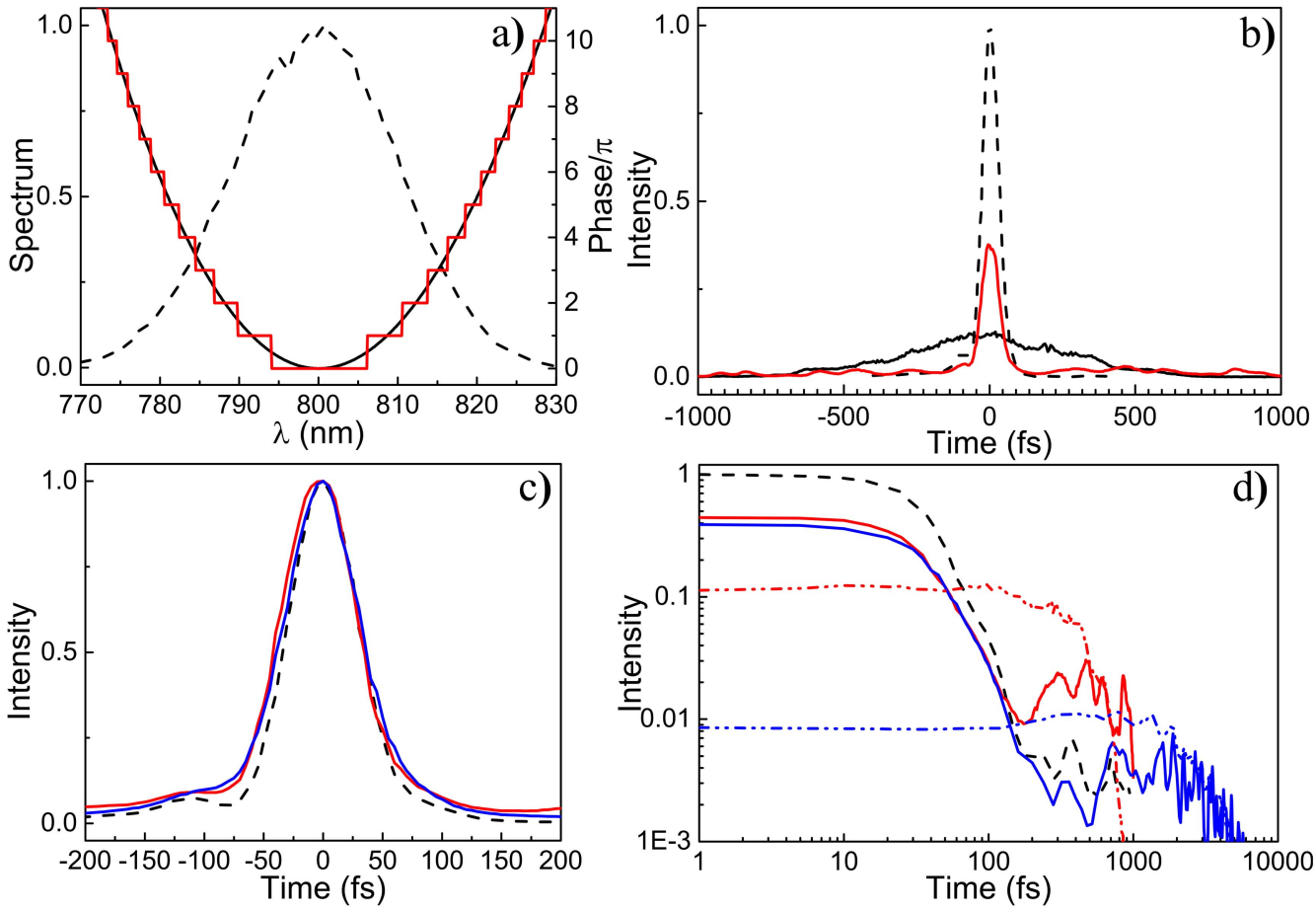

Figure 2. Experimental results (a) spectrum and phases used to stretch the pulse 10 times using a chirp value of 10 000 fs^2 (black) and binary (red) phase added to compress it back to have FWHM as for TL pulse. (b) Cross-correlation functions of TL pulse (dashed) 10 times stretched (black) and binary compressed pulse (red). (c) Cross-correlation functions for TL pulse (dashed) and binary compressed pulse that is originally 10 times stretched (red) and 100 times stretched (blue) normalized on the maximum. (d) Long time behavior for TL (black dashed), chirped at 10 (red dashed) and 100 (blue dashed) times, and binary compressed pulses that were originally chirped at 10 (red) and 100 times (blue) on a log–log scale for positive delay times.

Fourier integral equation (2) for part of the spectrum between frequencies ω_1 and ω_2:

$$E(t)=\int_{\omega_1}^{\omega_2} e^{\frac{1}{2}(i\varphi''-\tau_0^2)\omega^2-i\omega t}d\omega=\frac{\sqrt{\pi/2}}{\tau_0\sqrt{1-i\varphi''\tau_0^{-2}}}\times e^{-\frac{t^2}{2\tau_0^2(1-i\varphi''\tau_0^{-2})}}\left[\mathrm{erf}\left(\frac{\omega_2(\varphi''+i\tau_0^2)-t}{\sqrt{2}\sqrt{i\varphi''-\tau_0^2}}\right)-\mathrm{erf}\left(\frac{\omega_1(\varphi''+i\tau_0^2)-t}{\sqrt{2}\sqrt{i\varphi''-\tau_0^2}}\right)\right]. \quad (8)$$

We can find the frequencies where the spectral phase is equal to $n\pi$, which depend on the applied chirp φ'' according to

$$\Omega_n=\sqrt{2\pi n/\varphi''}. \quad (9)$$

We now identify phases that are equal to π or 0 between frequencies Ω_n^- and Ω_n^+ for even and odd n, correspondingly:

$$\Omega_n^-=\sqrt{2\pi(n-0.5)/\varphi''},\ \Omega_n^+=\sqrt{2\pi(n+0.5)/\varphi''}. \quad (10)$$

It is possible to calculate the total electric field using equation (8). Results of these calculations are shown in figure 3(1). The first panel 3(1)(a) shows the Gaussian spectrum with carrier frequency ω_0 (dashed line) together with the stretching quadratic phase modulation (black) and binary phase to compress stretched pulse (red). The calculated intensities of the corresponding electric fields are shown in 3(1)(b), presented in log–log scale for positive time. The pulse is stretched 50 times its original duration by chirp in this example; its peak intensity drops 50 times as shown in figure 3(1)(b). Because both the spectrum and the phases applied are symmetric, we only plot the positive half. The reader should keep in mind that the 'tail' of the pulse and 'pre-pulse' are identical. The binary-phase compressed

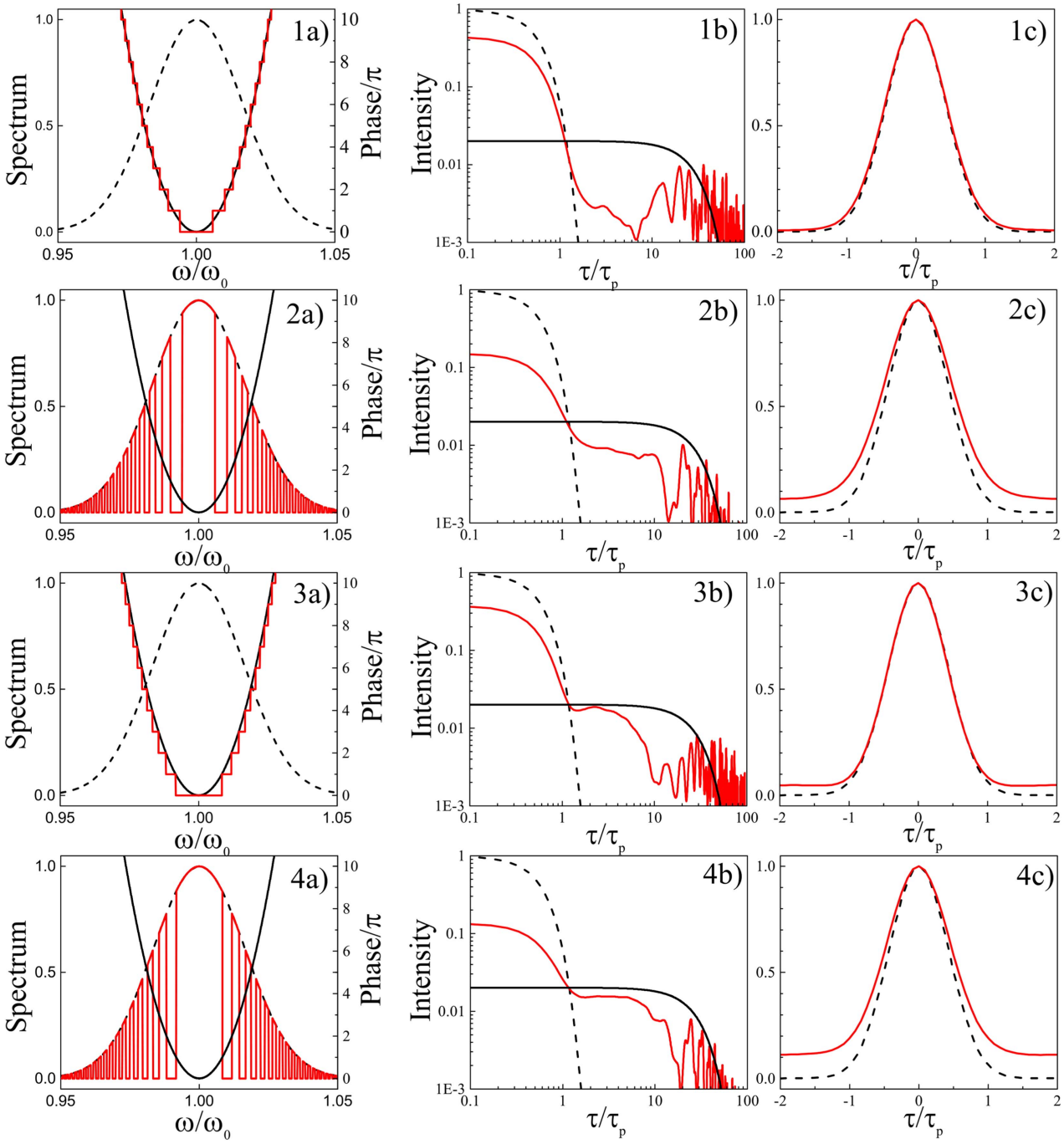

Figure 3. Different methods of pulse compression. (a) (*x*-axis is relative to carrier frequency) Spectrum (dashed) with parabolic phase (black) dispersion to stretch the pulse, and phase (or amplitude) to compensate back to TL duration (red). (b) (*x*-axis is ratio of time to the duration of the pulse) Plots of TL (dashed), chirped (black) and compressed (red) pulses on log–log scales to show how laser energy is distributed in time. (c) Intensities of TL (dashed) and compressed (red) pulses normalized on maxima to show compression quality. Cases (1) and (3) pure phase and (2) and (4) amplitude compression of Gaussian spectrum with linear chirp. (1) and (2) using optimal binary-phases equations (3), (4) and (10) using phase and amplitude modulations defined by classical Fresnel zones equation (9).

pulse has a peak intensity of ∼0.4 relative to TL. In panel 3(1)(c), we show the time profiles of the TL pulse and the binary compressed pulse, which are very close one to another, with pulse and duration of the binary compressed pulse practically equal to the duration of the TL pulse.

The second row of results in figure 3(2) presents results where instead of using binary-phase modulation we eliminate those spectral components, setting their amplitude to zero. The binary amplitude compression successfully produces short pulses; however, the resulting peak amplitude of the compressed pulse is less than 0.15 relative to TL. Moreover, additional background appears giving these pulses much lower contrast. We learn that phase compression is more efficient than amplitude modulation because we are able to turn destructive interference into constructive interference.

The third and fourth rows, figures 3(3) and (4), present results of phase and amplitude modulation using slightly different zones with direct analogy to the classical Fresnel zones used for spatial focusing. When spectral components with phase delays relative to the central one are less than $n\pi$, they are phase shifted or eliminated. Again, we can see the pure phase modulation is more effective than amplitude modulation. We also see that this method is slightly less efficient than the approach described in section 1, and pulse compression is not as good (compare row 3.1 to row 3.3).

4.2. Compression of different phases

In the previous subsection, we showed the efficient compression of linearly chirped pulses with a Gaussian spectrum. In this section, we apply this method for pulses with different spectra and different phase distortions. The formula used to calculate the binary-phase compression for any frequency ω is relatively simple:

$$\varphi(\omega) = \pi \times \text{round}[\varphi(\omega)/\pi]. \tag{11}$$

We explore five different cases: first, in figure 4(1), pulses with a Gaussian spectrum are stretched 100 times using linear chirp. Second, in figure 4(2), a third order (cubic) phase mask was applied to stretch the pulse by a factor of 100. Third, in figure 4(3), pulses with a Gaussian spectrum are stretched to get a square pulse in the time domain using nonlinear phase modulation by the method reported by Lozovoy *et al* [11]. Fourth, in figure 4(4), the pulses have a flat-top spectrum and are stretched by chirp. Lastly, in figure 4(5), pulses with a non-Gaussian (double Gauss) spectrum with a complex phase that is composed of both second and third order dispersions. The results from binary-phase compression are remarkable. Independent of pulse spectrum and the type of phase used for stretching, all pulses are compressed back to their TL duration, with an intensity time profile identical to that before stretching. In all cases, the peak intensity of the compressed pulses is ~0.4 relative to TL.

4.3. Compression of highly stretched pulses

In this subsection, we explore the theoretical limits of binary-phase compression. In particular, we explore how binary-phase compression behaves when compressing highly stretched pulses. Results from our calculations are shown in figure 5. Note that for pulses stretched by more than a factor of 100, the resulting pulse duration is essentially the same as the original TL pulse and the amplitude approaches 0.4 relative to TL. Table 1 summarizes these results. Pulses were stretched from 1 to 6 orders of magnitude. Their relative pulse duration with respect to TL approaches unity. The peak intensity of the compressed pulses approaches 0.40 compared to the original TL pulse. We learn that the greater the stretching factor is, the better the binary-phase compression approach performs.

4.4. Quality of the compressed pulses

Given the excellent experimental results, we consider how imperfections in the implementation of binary-phase compression affect the quality of the compressed pulses using two parameters to characterize deviations from the optimum TL pulse target. We consider the compression ratio (τ/τ_0), where 1.0 is considered perfect, and amplitude (I/I_0), which is the ratio between the peak intensity of the compressed pulse using 'perfect' binary-phase compression, remembering $I_0 \approx 0.4I_m$ where I_m is peak intensity of the fully compressed pulse, and imperfect binary-phase compression. In particular, we study the following five imperfections, and the results of our analysis are summarized in figure 6. First, when a systematic error in accuracy $\Delta\varphi$ is introduced in the value of π (figure 6(1)). Second, when a random error in the precision $\delta\varphi$ in the phase value of π is introduced at each pixel (figure 6(2)). Third, when the spectral resolution Δ of the device used to introduce the spectral phase is limited (figure 6(3)). Fourth, when the number of phase steps (pixels in a 4-f shaper) is limited (figure 6(4)). Fifth, when the binary-phase compression is designed for a value of chirp that is different from the chirp used for stretching (figure 6(5)).

The optimal phase for binary compression (black line) is plotted along with the imperfect phase (red line). The first panels (a) show the total spectral phase, i.e. the chirp required to stretch the pulses by a factor of 100 and the binary-phase applied for compression. This is why the phases in figure 6 look like a 'saw tooth' and not like a 'staircase'. Because phase is a cyclic parameter with period 2π we plot the wrapped phase. Panels (b) show how the compression quality degrades as a function of increasing the imperfection being tested. Black points give the compression quality (τ/τ_0) and open points are the intensity (I/I_0).

In figure 6(1), we consider the effect of using an imperfect value of π. Here we use 1.5π. Interestingly, deviations from π do not affect the compressed pulse duration, and only the peak intensity of the compressed pulse is affected. As long as the phase inaccuracy is less than 0.1π even the amplitude of the compressed pulse is not affected. In figure 6(2), we analyze the effect of random phase fluctuations. Not surprisingly, the results are very similar to those in figure 6(1). We learn that accuracy and precision behave similarly, and as long as phase precision and accuracy are within 0.1π, compression and amplitude are unaffected.

In figure 6(3), we analyze the limited spectral resolution Δ of the phase steps. Surprisingly, spectral resolution does not decrease the quality of the compression in terms of duration or intensity. Moreover, limited resolution suppresses the temporal wings of the output pulse. Mathematically it is a consequence of the convolution theorem; limited spectral resolution suppresses temporal components far from the pulse. In fact, this effect can be used to 'clean up' the pulse.

In figure 6(4), we analyze the limitation in the number of phase steps or pixels when using a pixelated pulse shaper. For these calculations we evaluate results starting from 500 intervals (pixels) and reduce to 100 across the entire spectrum (within $\pm 0.1\omega_0$). We find that as long as the number of

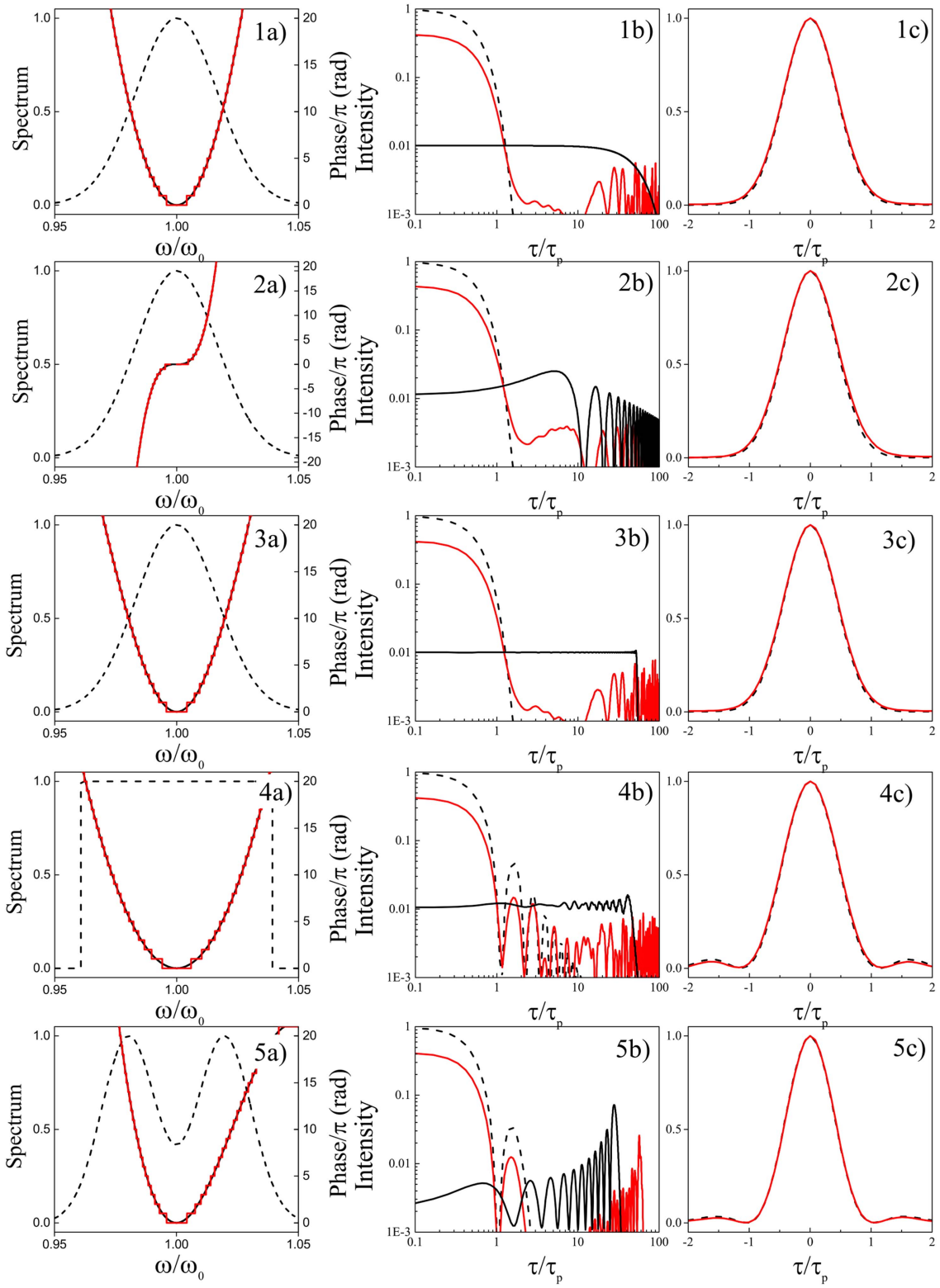

Figure 4. Compression of different pulses. (a) (*x*-axis is relative to carrier frequency) Spectrum (dashed) with parabolic phase (black) dispersion to stretch the pulse, and amplitude of phase (red) to compensate back to TL duration. (b) (*x*-axis is the ratio of time to the duration of the pulse) Plots of TL (dashed), chirped (black) and compressed (red) pulses on log–log scales to show how laser energy is distributed in time. (c) Intensities of TL (dashed) and compressed (red) pulses normalized on maxima to show compression quality. Cases evaluated: (1) Gaussian spectrum with linear chirp; (2) Gaussian spectrum with third order (cubic) dispersion; (3) Gaussian spectrum with nonlinear chirp to generate a square pulse in the time domain; (4) square spectrum with linear chirp; (5) complex spectrum (double Gauss) with nonlinear phase dispersion (sum of quadratic and cubic phases).

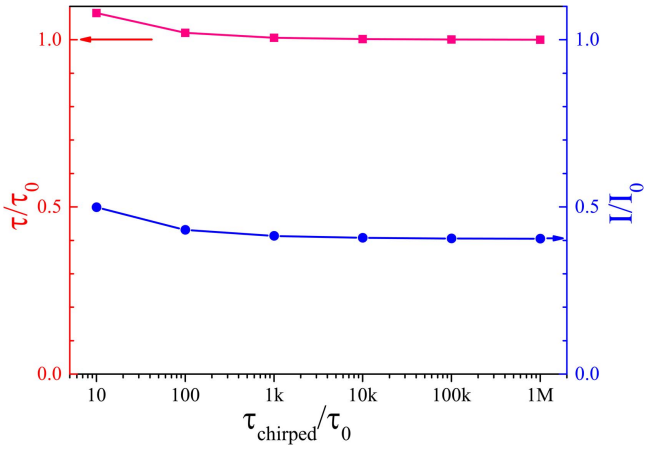

Figure 5. Dependence of compression and efficiency from duration of stretched pulse.

Table 1. Compression of pulses with different initial stretching.

Stretching	(Duration)/(TL Duration)	(Intensity)/(TL Intensity)
10	1.080	0.4987
10^2	1.021	0.4311
10^3	1.006	0.4131
10^4	1.002	0.4077
10^5	1.001	0.4053
10^6	1.000	0.4051

intervals equals the stretching factor there is little or no degradation of the compression quality in time or intensity.

Finally, in figure 6(5), we analyze the case in which the binary-phase mask is designed for a different compression factor. We find that a 1% difference in the stretched pulse duration results in a compressed pulse that is 30% longer than the original with an intensity that is 20% lower as in the shown example where a pulse that was stretched 101 times is being compressed using a binary mask that is designated for a stretching factor of 100. This sensitivity is very significant and implies that practical implementations will require some level of fine adjustment. This is typically available in the stretcher of ultrafast lasers.

4.5. High-contrast compressed pulses

While binary phase compression performs quite well, 60% of the pulse energy ends up as a pre- and post-pulse pedestal. Here, we address how to eliminate this pedestal, given that one of the most important parameters of pettawatt and higher energy laser pulses is the contrast ratio of the pulses, which is defined as the ratio between the peak intensity of the pulse to the pre-pulse intensity. The reason for requiring a high contrast is that most atoms and molecules ionize at peak laser intensities of $10^{14}\,\mathrm{W\,cm^{-2}}$, therefore a laser pulse such as those shown so far, with contrast ratios of 10^{-2}, would pre-ionize the target well ahead of the main pulse arrival, such that plasma expansion would obscure the interaction with the main pulse. The pre-ionization time can be greatly shortened by increasing the contrast ratio of the pulses. Experiments in the relativistic optics regime and higher require contrast ratios between 9 and 10 orders of magnitude. From the different approaches that have been demonstrated for improving the contrast ratio of intense femtosecond pulses, we consider the plasma mirror and cross-polarized wave generation (XPW). The plasma mirror approach takes advantage of the plasma formed on the surface of a dielectric placed in vacuum. When the intensity of the incident pulse is low it transmits through the dielectric, however, when the intensity is sufficiently high it becomes reflective in what is known as a self-shuttering effect [17, 18]. Usually, the plasma mirror method achieves a two-order of magnitude improvement in the contrast ratio of the leading edge of the pulses with transmission reaching 70% [19]. Higher contrast ratios can be reached by a double plasma mirror arrangement [20].

A second method for increasing the contrast ratio of high-energy laser pulses is XPW, where a strong linear polarized pulse generates perpendicular polarized light through third-order nonlinear optical process in a crystal. The weak background wings generate much smaller perpendicularly polarized signal, therefore the expected contrast ratio of XPW would be in a cubic order with respect to the original stretching factor with an experimental active efficiency of up to 25% [21, 22]. While XPW was first introduced to reduce amplified spontaneous emission (ASE) from high-energy laser pulses, here we calculate if the same suppression that is observed for ASE can suppress the temporally dispersed signals arising from binary-phase compression. The formula used to calculate the XPW field is

$$E_{\mathrm{XPW}}(t) \propto \chi^{(3)} E(t) E^{*}(t) E(t). \tag{12}$$

Results of calculations incorporating XPW for pulses with initial temporal chirp-stretching 10^2 (a), 10^3 (b) and 10^4 (c), are shown in figure 7. The black lines correspond to the time profile of the initially stretched pulses followed by binary-phase compression. The red lines correspond to the same pulses after XPW filtering. For pulses initially stretched 100 times (figure 7(a)), the contrast ratio improves by 10^2 and the cleaned pulses have a contrast better than 10^6. For pulses initially stretched by a factor of 1000 (figure 7(b)), the contrast after XPW is then better than 10^9. For pulses stretched by 10^4 (figure 7(c)), as would be used in a CPA system, XPW increases the contrast by about eight orders of magnitude. The binary-phase compressed and XPW filtered pulses achieve a contrast of 10^{12}. The dependence of XPW filtering on initial stretching can be explained as a function of how spread out are the dispersed components that are not compressed by the coarse choice of phases (0 and π). Greater initial stretching leads to greater spreading, which implies greater contrast gain. In addition to the improved contrast ratio, we see that the third-order dependence of XPW leads to some pulse compression beyond the original TL.

5. Discussion and conclusions

The experimental and numerical analysis presented on binary-phase compression has taught us several important

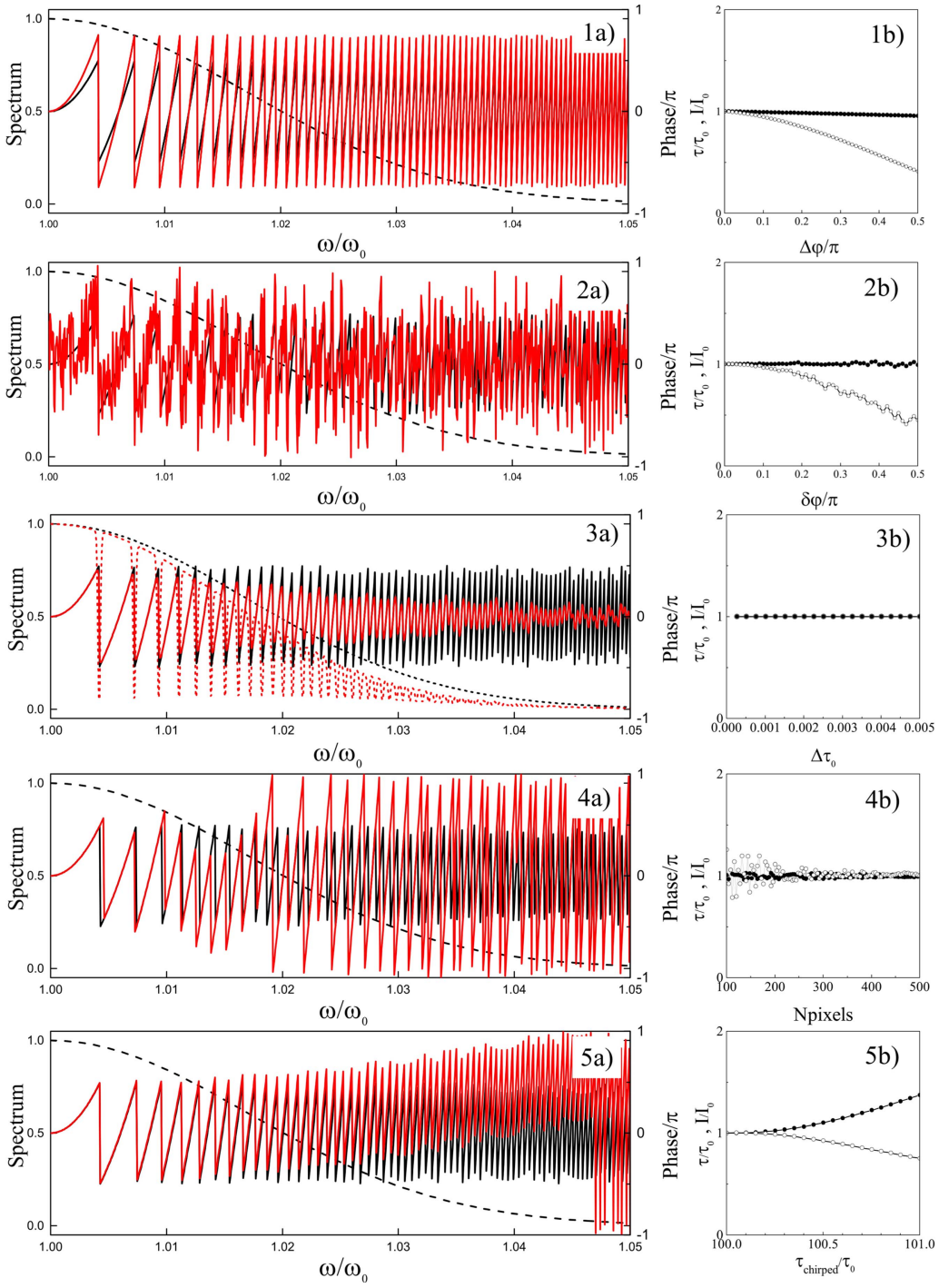

Figure 6. Quality of binary phase compression for a pulse stretched by a factor of 100 by chirp and compressed using a binary-phase function with different imperfections. The first column (column a) shows the Gaussian spectrum (black dashed line), the ideal phase of the compressed pulse (black line), and the imperfect phase (red line). Note that only the high frequency half of the spectrum is shown, the laser spectrum and compression phase are symmetric in the frequency domain. Case 1 considers deviations in phase accuracy, 1.5π instead of π; panel 1(b) shows how the compression is unaffected, however the amplitude ratio degrades as the deviation from pi increases from 0 to 0.5π. Case 2 considers deviations in phase precision, with fluctuations from 0 to π; panel 2(b) shows how the compression quality remains unaffected, however the amplitude ratio degrades as the precision degrades from 0 to 0.5π. Case 3 considers limited spectral resolution, which affects the amplitude of the spectrum (red pointed line) but not the compression; panel 3(b) shows how compression quality is not affected by spectral resolution. Case 4 considers a limited number of frequency intervals (pixels describing the phase mask); panel 4(b) shows how the compression quality is not affected by the number of frequency intervals as long as the number is the same or greater than the stretching factor. Case 5 considers the performance of binary-phase compression when the phase mask is designed for a compression factor different from the actual stretching; panel 5(b) shows how the quality of compression degrades as the chirped pulse exceeds the factor of 100 stretching.

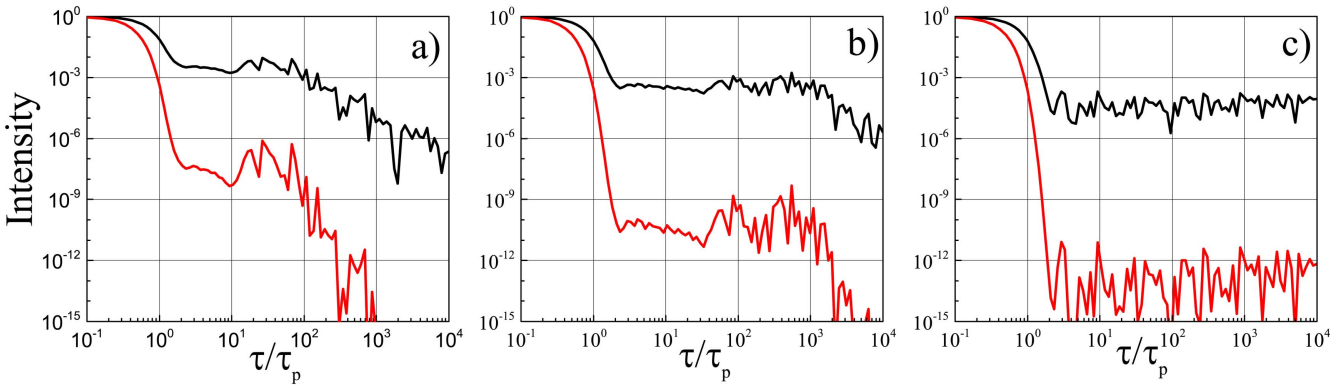

Figure 7. XPW filtering to improve contrast ratio by over seven orders of magnitude. Calculated temporal profiles of binary-phase compressed pulses before (black) and after XPW-filtering (red) in log–log scales for initially chirped stretching by (a) 10^2, (b) 10^3 and (c) 10^4 times.

lessons. First, the performance of binary-phase compression depends primarily on the proper spacing of the phase steps, and not their sharpness or the accuracy and precision of the phase value. This observation reminds us of the analogy between the time domain (binary-phase compression) and the spatial domain (diffraction gratings). The performance of gratings depends on the spacing between the grooves and not the shape of the features. Second, we find that the performance of binary-phase compression is independent of the laser pulse spectrum, and it can be used to compress pulses with chirp and third-order dispersion and we see no reason why not higher orders as well. The main drawback we find for binary-phase compression is that the spacing between steps needs to closely match (within a few percent) the phase being compensated. This implies that for fixed binary-phase masks, it will be important to have a means to make small phase adjustment. This could be achieved with a pair of prisms, gratings or a pulse shaper placed before the main power amplifier.

In terms of implementation, we have shown successful experimental results using a programmable pulse shaper. However, chirp pulse amplification laser systems require stretching and compression factors of four to five orders of magnitude. For such levels, programmable pulse shapers are not presently practical. Given that pulse compressors for petawatt and exawatt ultrafast lasers require optics exceeding one meter squared placed in large vacuum chambers, there is an incentive to consider the implementation of approaches that do not require conventional gratings. We do not propose the use of pulse shapers to compress amplified pulses. Here we suggest that maximum advantage of the method proposed would be achieved by its implementation in a single optic such as a volume Bragg grating or a multilayer dielectric mirror. For example, in a previous project we have found that a New Focus NIR5102 mirror, having a pair of multilayer high-reflectance coatings, introduces discontinuous phase jumps that stretch a 15 fs pulse to a pulse duration exceeding 200 fs. We were able to recompress the pulse back to its TL pulse duration after compensation of the phase distortions introduced by the mirror [23]. We can think of reversing the experiment and using the mirror as a single reflection compressor and the pulse shaper as the stretcher.

To control the steepness of the spectral-phase steps required for the approach presented here the concept of 'apodization' can be used [13]. To achieve alternation of 0 and π spectral phase or amplitude modulation, analogous to multi-spectral notch interference filters, a smooth modulation of the index of refraction can be used [24]. We think it will be possible to create single-optic compressors because, as shown in the paper, to compress a pulse N times we need approximately a spectral phase function with N phase points or N layers [25]. Multilayer optics are now reaching maturity and programmable systems to create them are available to some of the larger laser companies. In terms of the final contrast ratio, we have found that binary-phase compression combines well with XPW filtering, and can lead to high contrast pulses.

In summary, we introduce a radical new approach to pulse compression based on the introduction of a coarse binary spectral phase. We find this approach can be used to compress highly stretched pulses back to their TL pulse duration. We have demonstrated the approach experimentally, with results that are in close agreement with numerical calculations. Finally, we show that binary-phase compression is highly compatible with XPW filtering, and can lead to high-contrast ultrafast pulses.

Acknowledgments

The authors are grateful for the financial support of this work from the Chemical Sciences, Geosciences and Biosciences Division, Office of Basic Energy Sciences, Office of Science US Department of Energy, DOE SISGR (DE-SC0002325). We thank Dr Christopher Mancuso for insightful suggestions regarding our manuscript. We also would like to thank Patrick Pawlaczyk for proofreading the manuscript.

ORCID iDs

Vadim V Lozovoy https://orcid.org/0000-0003-2129-3570
Muath Nairat https://orcid.org/0000-0002-6384-584X
Marcos Dantus https://orcid.org/0000-0003-4151-5441

References

[1] Strickland D and Mourou G 1985 *Opt. Commun.* **56** 219–21
[2] Broers B, Noordam L D and van Linden van den Heuvell H B 1992 *Phys. Rev.* A **46** 2749–56
[3] Myers O E 1951 *Am. J. Phys.* **19** 359–65
[4] Sussman M 1960 *Am. J. Phys.* **28** 394–8
[5] Lit J W Y and Tremblay R 1970 *Can. J. Phys.* **48** 1799–805
[6] Weiner A M 2011 *Opt. Commun.* **284** 3669–92
[7] Xu B, Gunn J M, Cruz J M D, Lozovoy V V and Dantus M 2006 *J. Opt. Soc. Am.* B **23** 750–9
[8] Coello Y, Lozovoy V V, Gunaratne T C, Xu B, Borukhovich I, Tseng C-H, Weinacht T and Dantus M 2008 *J. Opt. Soc. Am.* B **25** A140–50
[9] Lozovoy V V, Xu B, Coello Y and Dantus M 2008 *Opt. Express* **16** 592–7
[10] Rasskazov G, Ryabtsev A, Lozovoy V V and Dantus M 2016 *Opt. Lett.* **41** 131–4
[11] Lozovoy V V, Rasskazov G, Ryabtsev A and Dantus M 2015 *Opt. Express* **23** 27105–12
[12] Jullien A *et al* 2005 *Opt. Lett.* **30** 920–2
[13] Szipőcs R and Kőházi-Kis A 1997 *Appl. Phys.* B **65** 115–35
[14] Chang G, Rever M, Smirnov V, Glebov L and Galvanauskas A 2009 *Opt. Lett.* **34** 2952–4
[15] Zhang H, Tang D Y, Zhao L M and Tam H Y 2008 *Opt. Lett.* **33** 2317–9
[16] Zhang H, Tang D Y, Zhao L M, Wu X and Tam H Y 2009 *Opt. Express* **17** 455–60
[17] Kapteyn H C, Szoke A, Falcone R W and Murnane M M 1991 *Opt. Lett.* **16** 490–2
[18] Gold D M 1994 *Opt. Lett.* **19** 2006–8
[19] Doumy G, Quéré F, Gobert O, Perdrix M, Martin P, Audebert P, Gauthier J C, Geindre J P and Wittmann T 2004 *Phys. Rev.* E **69** 026402
[20] Lévy A *et al* 2007 *Opt. Lett.* **32** 310–2
[21] Chvykov V, Rousseau P, Reed S, Kalinchenko G and Yanovsky V 2006 *Opt. Lett.* **31** 1456–8
[22] Cotel A, Jullien A, Forget N, Albert O, Chériaux G and Le Blanc C 2006 *Appl. Phys.* B **83** 7–10
[23] Pestov D, Lozovoy V V and Dantus M 2010 *Opt. Lett.* **35** 1422–4
[24] Bovard B G 1993 *Appl. Opt.* **32** 5427–42
[25] Kashyap R 2010 *Fiber Bragg gratings* (London: Academic)